Clin Orthop Relat Res (2015) 473:1830–1839
DOI 10.1007/s11999-015-4154-8

Clinical Orthopaedics and Related Research®
A Publication of The Association of Bone and Joint Surgeons®

BASIC RESEARCH

Low-intensity Pulsed Ultrasound Enhances Bone Repair in a Rabbit Model of Steroid-associated Osteonecrosis

Hanxiao Zhu MD, Xunzi Cai MD, Tiao Lin MD, Zhongli Shi MD, Shigui Yan MD

Received: 29 July 2014 / Accepted: 13 January 2015 / Published online: 4 March 2015

Abstract

Background Steroids are a leading cause of femoral head osteonecrosis. Currently there are no medications available to prevent and/or treat steroid-associated osteonecrosis. Low-intensity pulsed ultrasound (LIPUS) was approved by the FDA for treating delayed union of bone fractures. Some studies have reported that LIPUS can enhance bone formation and local blood flow in an animal model of fracture healing. However, whether the effect of osteogenesis and neovascularization by LIPUS can enhance the repair progress in steroid-associated osteonecrosis is unknown.

Questions/purposes We hypothesized that LIPUS may facilitate osteogenesis and neovascularization in the reparative processes of steroid-associated osteonecrosis. Using a rabbit animal model, we asked whether LIPUS affects (1) bone strength and trabecular architecture; (2) blood vessel number and diameter; and (3) BMP-2 and VEGF expression.

Methods Bilateral femoral head necrosis was induced by lipopolysaccharide and methylprednisolone in 24 rabbits. The left femoral heads of rabbits received LIPUS therapy (200 mW/cm^2) for 20 minutes daily and were classified as the LIPUS group. The right femoral heads of the same rabbits did not receive therapy and were classified as the control group. All rabbits were euthanized 12 weeks after LIPUS therapy. Micro-CT, biomechanical testing, histologic evaluation, immunohistochemistry, quantitative real-time PCR, and Western blot were used for examination of the effects of LIPUS.

Results Twelve weeks after LIPUS treatment, the loading strength in the control group was 355 ± 38 N (95% CI, 315–394 N), which was lower ($p = 0.028$) than that in the LIPUS group (441 ± 78 N; 95% CI, 359–524 N). The bone tissue volume density (bone volume/total volume) in the LIPUS group (49.29% ± 12.37%; 95 % CI, 36.31%–62.27%) was higher ($p = 0.022$) than that in the control group (37.93% ± 8.37%; 95 % CI, 29.15%–46.72%). The percentage of empty osteocyte lacunae in the LIPUS group (17% ± 4%; 95% CI, 15%–20%) was lower ($p = 0.002$) than that in the control group (26% ± 9%; 95% CI, 21%–32%). The mineral apposition rate (μm/day) in the LIPUS group (2.3 ± 0.8 μm/day; 95% CI, 1.8 2.8 μm/day) was higher ($p = 0.001$) than that in the control group (1.6 ± 0.3 μm/day; 95% CL, 1.4–1.8 μm/day). The number of blood vessels in the LIPUS group (7.8 ± 3.6/mm^2; 95% CI, 5.5–10.1 mm^2) was greater ($p = 0.025$) than the number in

Hanxiao Zhu and Xunzi Cai contributed equally to this work and should be considered as co-first authors.

The institution of the authors has received funding from the National Natural Science Foundation of China (Hangzhou, Zhejiang, China) (81101377, 81101345, 81171687, 81371954, 81201414, 81201416, 81401785, 81472113); The Key Project of Zhejiang Provincial Department of Science and Technology (Hangzhou, Zhejiang, China) (2011C13033); Zhejiang Provincial Natural Science Foundation of China (Hangzhou, Zhejiang, China) (Y2100161, Y2110239); and The Fund of Health Department of Zhejiang Province (Hangzhou, Zhejiang, China) (2012RCA032).
All ICMJE Conflict of Interest Forms for authors and *Clinical Orthopaedics and Related Research*® editors and board members are on file with the publication and can be viewed on request.
Clinical Orthopaedics and Related Research® neither advocates nor endorses the use of any treatment, drug, or device. Readers are encouraged to always seek additional information, including FDA-approval status, of any drug or device prior to clinical use.
Each author certifies that his or her institution has approved the animal protocol for this study and that all experiments were conducted in conformity with ethical principles or research.

H. Zhu, X. Cai, T. Lin, Z. Shi, S. Yan (✉)
Department of Orthopaedic Surgery, Second Affiliated Hospital's Campus in Binjiang District, School of Medicine, Zhejiang University, No. 88 Jiefang Road, Hangzhou 310009, People's Republic of China
e-mail: zrjwsj@zju.edu.cn; zhuhanxiao@zju.edu.cn

the control group (5.7 ± 2.6/mm^2; 95% CI, 4.0–7.3 mm^2). Messenger RNA (mRNA) and protein expression of BMP-2 in the LIPUS group (75 ± 7, 95% CI, 70–79; and 30 ± 3, 95% CI, 28–31) were higher (both $p < 0.001$) than those in the control groups (46 ± 5, 95% CI, 43–49; and 15 ± 2, 95% CI, 14–16). However, there were no differences ($p = 0.114$ and 0.124) in mRNA and protein expression of vascular endothelial growth factor between the control (26 ± 3, 95% CI, 24–28; and 22 ± 6, 95% CI, 18–26) and LIPUS groups (28 ± 2, 95% CI, 26–29; and 23 ± 6, 95% CI, 19–27).

Conclusions The results of this study indicate that LIPUS promotes osteogenesis and neovascularization, thus promoting bone repair in this steroid-associated osteonecrosis model.

Clinical Relevance LIPUS may be a promising modality for the treatment of early-stage steroid-associated osteonecrosis. Further research, including clinical trials to determine whether LIPUS has a therapeutic effect on patients with early-onset steroid-associated osteonecrosis may be warranted.

Introduction

Approximately 20,000 patients per year are diagnosed with femoral head osteonecrosis in the United States [23]. Steroids, commonly prescribed to patients with systemic lupus erythematosus, nephrotic syndrome, or organ transplantation, are a leading cause of femoral head osteonecrosis; this is known as steroid-associated osteonecrosis [1, 35, 41]. Once osteonecrosis begins, 80% of femoral heads will collapse if no treatment is administered [32]. Steroid-associated osteonecrosis can lead to social and family burdens, especially because these patients often are young. The patients with collapse of the femoral head often require THA. In addition, despite progress with THA, some of these patients need revision surgery owing to their young age at the time of the primary surgery, and have low functional scores [25]. Consequently, emphasis has been placed on preventing irreversible complications after steroid-associated osteonecrosis such as biomechanical collapse of the femoral head and osteoarthritis [1].

To date, there is no known effective treatment for an uncollapsed femoral head owing to steroid-associated osteonecrosis. This is partially because the exact pathophysiology of steroid-associated osteonecrosis is unclear. It is thought that steroids interrupt blood flow by damaging the endothelial cells and altering lipid metabolism, leading to the production of fat emboli [4, 17, 18, 22]. Studies have shown that bone repair during the early stages of steroid-associated osteonecrosis is inadequate owing to the decreased activity of osteoblasts and bone marrow-derived stem cells after lengthy periods of steroid treatment [5, 35].

Low-intensity pulsed ultrasound (LIPUS) uses acoustic waves and is noninvasive. It has been approved by the FDA as a feasible, cost-effective method for treating delayed union and/or nonunion of bone fractures. The benefits of LIPUS have been documented during all stages of bone repair, including osteogenesis, angiogenesis, and chondrogenesis [28, 29]. In vitro studies have shown that LIPUS increases bone formation, osteoblast activity, and osteogenic differentiation of mesenchymal stem cells (MSCs) [27, 31]. In vivo studies have found that LIPUS treatment promotes new bone formation and improves tissue blood flow [3, 16, 24, 34]. Rutten et al. [29], in a clinical study, showed that LIPUS accelerates fracture healing through increased osteoblast activity. However, whether LIPUS can enhance the repair progress in steroid-associated osteonecrosis is unknown. As osteogenesis and neovascularization are key factors to enhance bone repair in osteonecrosis, we hypothesized that LIPUS may facilitate osteogenesis and neovascularization in the reparative processes of steroid-associated osteonecrosis.

Using a rabbit animal model, we asked whether LIPUS affects (1) bone strength and trabecular architecture; (2) blood vessel number and diameter; and (3) the messenger RNA (mRNA) and protein expression of BMP-2 and VEGF.

Materials and Methods

Overall Experimental Design

Bilateral femoral head necrosis was induced in New Zealand White rabbits (n = 24) through treatment with lipopolysaccharide (*Escherichia coli* 0111:B4; Sigma, St Louis, MO, USA) and methylprednisolone (Pharmacia and Upjohn, Puurs, Belgium). Lipopolysaccharide injection can induce a hypercoagulable and hypofibrinolytic state, which is similar to that in patients with systemic lupus erythematosus and nephrotic syndrome. LIPUS therapy was administered to the left femoral head of each rabbit 24 hours after lipopolysaccharide injection, and before the first methylprednisolone injection. The left femoral heads were designated the LIPUS group. Sham stimulation was administered to the right limbs (the device was turned off) and these were designated the control group. All animals were euthanized by a pentobarbital overdose 12 weeks after LIPUS therapy (Fig. 1). The proximal femurs were harvested and freed of soft tissue. Bilateral samples were taken from six randomly chosen rabbits and analyzed by micro-CT and mechanical testing. Samples from another six randomly chosen rabbits were used for Western blot analysis and quantitative real-time reverse transcriptase-PCR (QRT-PCR). The other 12 rabbits received intramuscular injections of a fluorescence tracer, calcein green (5 mg/kg; Sigma), and tetracycline hydrochloride (30 mg/kg; Sigma) at 14 and 4 days, respectively, before euthanasia to label newly

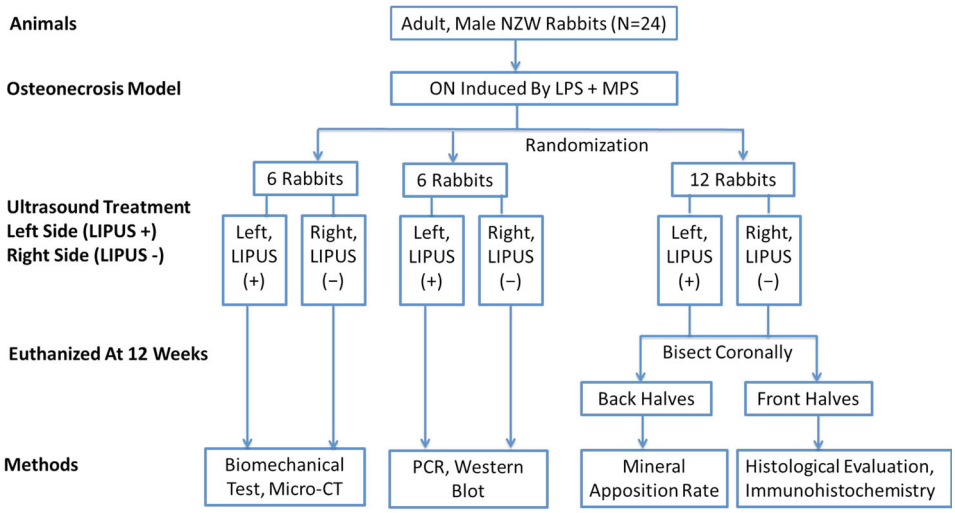

Fig. 1 The flow chart shows the study design. LIPUS = low-intensity pulsed ultrasound; NZW = New Zealand White rabbits; ON = osteonecrosis; LPS = lipopolysaccharide; MPS = methylprednisolone.

mineralized bone. The samples were bisected along the coronal plane. The anterior halves were used for histologic evaluation and immunohistochemistry and the posterior halves were prepared for evaluation of the mineral apposition rate.

Rabbit Model

Twenty-four adult male New Zealand White rabbits, weighing 2.7 to 3.0 kg, were used. The experimental protocol was approved by the Animal Care and Use Committee of Zhejiang University. Rabbits were fed a standard laboratory diet and water ad libitum. The steroid-associated osteonecrosis rabbit model was prepared using a previously published inductive protocol [26, 37]. Briefly, the rabbits received intravenous injections of 10 μg/kg lipopolysaccharide followed by intramuscular injections of methylprednisolone (20 mg/kg) 24 hours later. Two additional methylprednisolone injections then were administered at 24-hour intervals so that the rabbits received a total of three methylprednisolone injections. It has been reported that formation of osteonecrosis lesions can occur 2 weeks after methylprednisolone injection [26, 39]. Four animals were randomly selected for MRI (T1-weighted image, TR 400 ms, TE 20 ms; T2-weighted image, TR 2000 ms, TE 106 ms) 2 weeks after methylprednisolone injection to test whether osteonecrosis was induced.

Low-intensity Pulsed Ultrasound Treatment

An ultrasonic generator (US 13; Cosmogamma Co, Bologna, Italy) was used in this study. Our previous study found that 200 mW/cm^2 for 20 minutes per day effectively prevented periprosthetic osteolysis in the medullary canal of the rabbit femur [43]. In this study, rabbits were treated with a 1-MHz pulse frequency, 20% duty cycle, and 100-Hz repetition rate at an average intensity of 200 mW/cm^2 20 minutes per day for 12 weeks. Twenty-four hours after lipopolysaccharide injection, the first LIPUS treatment was administered before the first methylprednisolone injection. The stimulation parameters were calibrated by the manufacturer. The rabbits were anesthetized with 3% pentobarbital sodium before LIPUS treatment. The skin around the hip was cleaned and ultrasound gel (KL-250; Keppler Co, Hangzhou, China) was used to couple the LIPUS transmission.

Micro-CT Analysis

Both proximal parts of the bilateral femoral samples were prepared for micro-CT (eXplore Locus SP; GE Co, Fairfield, CT, USA) scanning, with a spatial resolution of 45 μm according to the protocol for animal studies. The structure of the trabecular bone in the volume of interest of the femoral head was evaluated with eXplore software [26, 35]. The mean volumetric bone mineral density (BMD) (mg/cc) and trabecular architectural parameters, including the bone tissue volume density (bone volume/total volume, %), trabecular number (expressed as 1/mm), trabecular thickness (expressed as μm), and trabecular spacing (expressed as μm) to define the degree of plate-like and rod-like trabecular bone in the femoral head were measured.

Biomechanical Evaluation

After micro-CT measurements, the loading strength of the femoral head was measured using an indentation test with a small-diameter (2.8 mm) indenter [15]. The proximal femurs were fixed and placed on the metal platform of a static

materials tester (Z2.5; Zwick/Roell, Ulm, Germany) and were tested in a wet condition. Alignment of the specimen was adjusted in accordance with the stainless steel rod in the upper holding device. The indenter was displacement-controlled at a constant rate of 5 mm/minute and was stopped when the load markedly decreased. Software (TestXpert II; Zwick/Roell) in the testing platform was used to automatically record the maximum bone strength (N).

RNA Extraction and QRT-PCR

The samples were mortared into powder under sterile conditions. Samples then were transferred to 1.5-mL Eppendorf centrifuge tubes. Total RNA was extracted using TRIzol® reagent (Invitrogen, Carlsbad, CA, USA) and precipitated in ethanol. The procedures were performed according to the manufacturer's instructions. The primers (Table 1) for QRT-PCR were designed by Oligo 6.0 primer design software (Molecular Biology Insights, Colorado Springs, CO, USA) and synthesized by Sangon Biotech (Sangon Biotech Co, Ltd, Shanghai, China). QRT-PCR was performed using a SYBR® Premix Ex Taq™ Kit (TaKaRa Biotech Co, Shiga, Japan). The data were collected by an iQ™5 detection system (Bio-Rad, Hercules, CA, USA) to calculate the cycle threshold (Ct) value of all samples. The relative quantifications of the gene expressions (BMP-2 and VEGF were calculated by the formula $2^{\triangle\triangle Ct} \times 10^5$. $\triangle\triangle Ct = \triangle Ct_1 - \triangle Ct_2$. $\triangle Ct_1$ is the value of the housekeeping gene 18S and $\triangle Ct_2$ indicates the Ct value of the target gene [7, 32]. The results of each group are presented as mean ± SD.

Western Blot Analysis

Protein from rabbit femoral head tissues was isolated with radioimmunoprecipitation assay buffer (RIPA) lysis buffer (Sangon Biotech Co, Ltd). A total of 60 μg of protein was loaded for electrophoresis on sodium dodecyl sulfate-polyacrylamide gel (Keduo, Hangzhou, China). The proteins then were transferred to polyvinylidene fluoride membranes (Sangon Biotech Co, Ltd). Goat antibodies against BMP-2 and VEGF (Santa Cruz Biotech, Inc, Santa Cruz, CA, USA) were diluted to a concentration of 1:200. The working concentration of internal control β-actin antibody used was 1:2000. The antibodies were incubated for 12 hours at 4° C. Goat antirabbit immunoglobulin G-horseradish peroxidase secondary antibody was diluted to 1:5000 and incubated for 1 hour at room temperature. Super Signal® West Dura Extended Duration Substrate (Thermo Scientific, Rockford, IL, USA) was used to detect the signals. The images were analyzed with Bandscan 5.0 (Glyko Inc, Novato, CA, USA) to calculate the intensity of the bands. The ratio of the intensities of the target genes and β-actin bands was used to represent the level of protein expression [32]. The results of each group are presented as mean ± SD.

Histologic Evaluation and Immunohistochemistry

Specimens for histologic evaluation were fixed in a 10% buffered neutral formalin solution. After decalcification in 10% EDTA, the samples were embedded in paraffin. Five-micron sections were cut and stained with hematoxylin and eosin for evaluation of osteonecrosis and calculation of fat cell size. The α-smooth muscle actin (α-SMA) staining was used to assess the number and mean diameter of blood vessels [2, 3]. The undecalcified samples were fixed in 70% ethanol solution at 4° C for 2 days, embedded in methylmethacrylate, and cut into 10-μm slices. The labeled surface and interlabeled thickness were measured. The single-labeled surface, double-labeled surface, and interlabeled thickness were measured except in the necrotic areas. The data were used for the following calculations: mineralizing surface/bone surface = (1/2 single-labeled surface + double-labeled surface)/bone surface (expressed as a percent); and, mineral apposition rate = interlabeled thickness per 10 days (expressed as μm/day) [6, 35].

Two sections of each sample were collected, separated by approximately 300 μm. Two pathologists (JL, LX)

Table 1. Real-time PCR primers and conditions

Gene	Genebank accession	Primer sequences (5′ to 3′)	Size (base pairs)	Annealing (° C)
Rabbit BMP-2	NM 001082650	GGGGTGGAACGACTGGATTGT	117	64
		GTCTGCACGATGGCATGGTTAGT		
Rabbit VEGF	AY196796	GGGGGCTGCTGCAATGATGAAA	97	65
		GCTGGCCCTGGTGAGGTTTGAT		
Rabbit 18S	EU236696	GACGGACCAGAGCGAAAGC	119	64
		CGCCAGTCGGCATCGTTTATG		

GeneBank available at: http://www.ncbi.nlm.nih.gov/genbank.

examined the sections from each sample, in a blinded fashion, for each staining procedure. Five fields in the subchondral area of the femoral head on each section were chosen [33]. The first field was located at the approximate center of the femoral head and the remaining four fields were located on both sides of the first field with two fields on each side. The mean of the two sections from each sample was taken as the value of that sample. The following parameters were assessed: (1) 200 osteocyte lacunae were counted in each established field at × 200 magnification and then the percentage of the empty osteocyte lacunae was determined [33]; (2) the average diameter of the fat cells was measured in each field and the average diameter for fat cells of each animal was determined [26, 33]; (3) the number and diameter of blood vessels were measured and averaged for each sample based on the α-SMA staining slides [3]. The number of blood vessels was expressed per area of tissue (/mm^2); (4) the mineralizing surface and bone surface and mineral apposition rate (μm/day) were calculated as described in previous studies [6, 35]. The decalcified slices were examined using a light microscope (Olympus BX51, Tokyo, Japan) and the undecalcified slices were observed under a fluorescence microscope (Olympus IX71). Different fields per slice were converted to digital pictures and quantitative analysis was performed using Image-Pro® Plus 6.0 (Media Cybernetics Inc, Rockville, MD, USA). Histologically, the femoral head was considered necrotic when at least one of the following three signs was present: bone marrow cell necrosis, empty osteocyte lacunae, or any evidence of repair, such as the presence of granulation tissue, fibrosis, or appositional bone formation [33, 37].

Statistical Analysis

Outcome measures for the LIPUS and the control groups were compared. Statistical differences between the two groups were determined by paired t-tests. The 95% CI was determined. A p value less than 0.05 was considered statistically significant. Levene's test ($p \leq 0.05$) was used to confirm variance homogeneity of the population.

Results

Osteogenesis in the Femoral Heads

Micro-CT images indicated that the trabecular bone was more sparse in the subchondral bone in the control group (Fig. 2A) compared with the LIPUS group (Fig. 2B). The BMD in the LIPUS group (608.94 ± 79.25; 95% CI, 525.77–692.12 mg/cc) was higher ($p = 0.019$) than that in the control group (564.91 ± 75.91; 95% CI, 485.24–644.58 mg/cc). The mean rate value of bone volume and total volume in the LIPUS group (49.29% ± 12.37%; 95 % CI, 36.31%–62.27%) was higher ($p = 0.022$) than that in the control group (37.93% ± 8.37%; 95 % CI, 29.15%–46.72%). Trabecular number was higher ($p = 0.006$) in the LIPUS group (2.65 ± 0.1 mm; 95 % CI, 2.54–2.75 mm) than in the control group (2.29 ± 0.21 mm; 95 % CI, 2.06–2.56 mm). Trabecular spacing was lower ($p = 0.025$) in the LIPUS group (201.36 ± 53.30 μm; 95 % CI, 145.42–257.29 μm) than in the control group (262.29 ± 81.50 μm; 95 % CI, 176.75–347.82 μm). Trabecular thickness was greater ($p = 0.029$) in the LIPUS group (174.44 ± 22.13 μm; 95 % CI, 151.21–197.67 μm) than in the control group (158.32 ± 23.03 μm; 95 % CI, 134.16–182.5 μm). Loading strength of the femoral head in the LIPUS group (441 ± 78 N; 95 % CI, 359–524 N) was 25% greater ($p = 0.028$) than in the control group (355 ± 38 N; 95 % CI, 315–394 N) (Table 2).

Histologic observations of the control group limbs showed sparser trabecular bone with massive empty lacunae and few osteoblasts lining the surfaces surrounded by large marrow fat cells and a disordered architecture of marrow tissue (Fig. 3A–B). In contrast, no such changes were observed in the LIPUS group limbs in which there were few empty lacunas and smaller fat cells (Fig. 3C–D). Consistent with histologic observations, MRI showed evidence of edema in the proximal

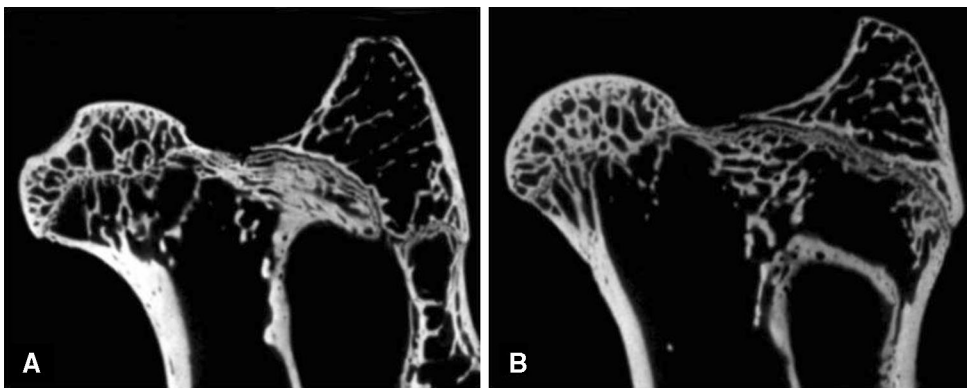

Fig. 2A–B (**A**) A representative micro-CT image from the control group showed that the trabecular bone was more sparse in the subchondral bone. (**B**) In the LIPUS group, the trabecular bone was thicker and denser.

Table 2. Biomechanical and histomorphometric evaluations and gene expression in the two groups

Outcome measures	Control (95% CI)	LIPUS (95% CI)	p value
Loading strength (N)	355 ± 38 (315–394)	441 ± 78 (359–524)	0.028*
Empty osteocyte lacunae (%)	26 ± 9 (21–32)	17 ± 4 (15–20)	0.002*
Fat cell diameter (μm)	35 ± 6 (31–38)	29 ± 5 (26–31)	0.023*
Mineralizing surface/bone surface (%)	62 ± 17 (51–73)	75 ± 16 (65–86)	0.001*
Mineral apposition rate (μm/day)	1.6 ± 0.3 (1.4–1.8)	2.3 ± 0.8 (1.8–2.8)	0.001*
Blood vessel number (/mm^2)	5.7 ± 2.6 (4.0–7.3)	7.8 ± 3.6 (5.5–10.1)	0.025*
Blood vessel diameter (μm)	21 ± 7 (17–26)	25 ± 7 (20–29)	0.215
BMP-2 mRNA	46 ± 5 (43–49)	75 ± 7 (70–79)	< 0.001*
BMP-2 protein	15 ± 2 (14–16)	30 ± 3 (28–31)	< 0.001*
VEGF mRNA	26 ± 3 (24–28)	28 ± 2 (26–29)	0.114
VEGF protein	22 ± 6 (18–26)	23 ± 6 (19–27)	0.124

Values are mean ± SD; *significant effect of LIPUS, $p < 0.05$; LIPUS = low-intensity pulsed ultrasound; mRNA = messenger RNA.

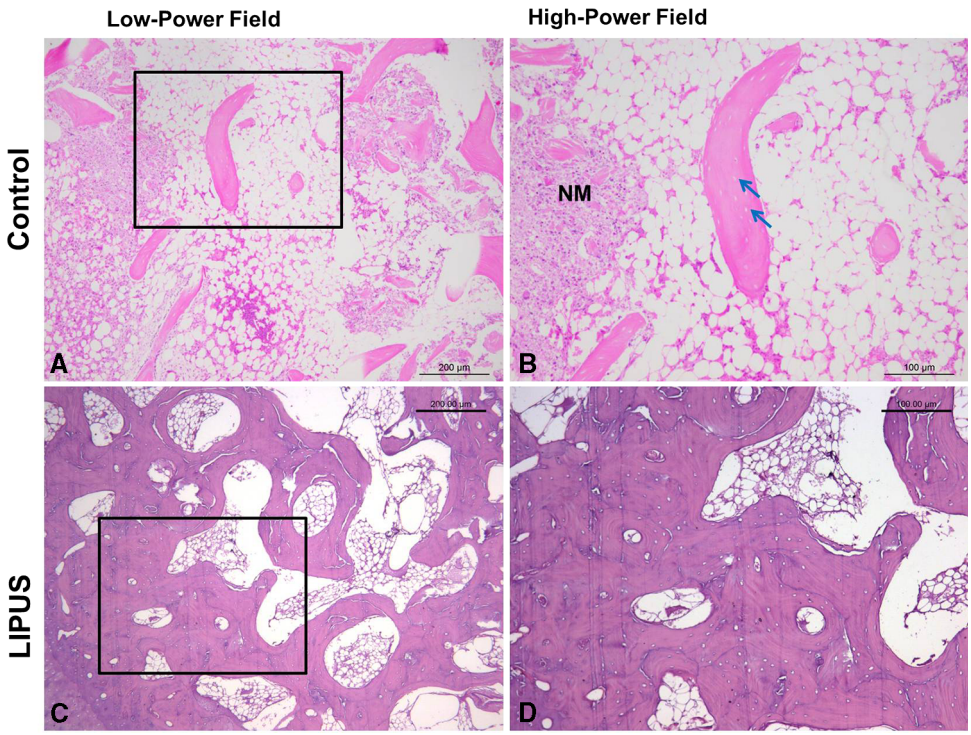

Fig. 3A–D (**A**) Enlarged fat cells, marrow necrosis necrotic bone, and massive empty osteocyte lacunae are shown in the control limbs (Original magnification, × 50). (**B**) The high-power field from the control group showed the empty lacunae (arrows) (Original magnification, × 100). (**C**) However, there are smaller fat cells, less bone and marrow necrosis, and fewer empty osteocyte lacunae in the LIPUS limbs (Original magnification, × 50). (**D**) The high-power field from the LIPUS group showed few empty lacunae (Original magnification, × 100).

femur (Fig. 4), which is identified as a potential cause of femoral head osteonecrosis [32]. The percentage of empty osteocyte lacunae in the LIPUS group (17% ± 4%; 95% CI, 15%–20%) was 51% lower ($p = 0.002$; Table 2) than in the control group (26% ± 9%; 95% CI, 21%–32%). The average fat cell diameter in the LIPUS group (29 ± 5 μm; 95% CI, 26–31 μm) was lower ($p = 0.023$) than that in the control group (35 ± 6 μm; 95% CI, 31–38 μm). Bone histomorphometric analyses also showed that the mineralizing surface/bone surface in the LIPUS group (75% ± 6%; 95% CI, 65%–86%) was increased ($p = 0.001$) compared with the control group (62% ± 17%; 95% CI, 51%–73%). The mineral apposition rate was higher ($p = 0.001$) in the LIPUS group (2.3 ± 0.8 μm/day; 95% CI, 1.8–2.8 μm/day) than in the control group (1.6 ± 0.3 μm/day; 95% CI, 1.4–1.8 μm/day).

Neovascularization in the Femoral Head

The α-SMA staining (Fig. 5) showed that the number of vessels in the LIPUS group (7.8 ± 3.6/mm^2; 95% CI, 5.5–10.1/mm^2) was higher ($p = 0.025$; Table 2) than in the

control group (5.7 ± 2.6/mm^2; 95% CI, 4.0–7.3/mm^2). However, the mean diameter of blood vessels was not different (p = 0.093) between the LIPUS group (25 ± 7 μm; 95% CI, 20–29 μm) and the control group (21 ± 7 μm; 95% CI, 17–26 μm). Enlarged fat cells were observed to be compressing blood vessels in the control group (Fig. 5A), which could lead to a decrease in blood perfusion.

BMP-2 and VEGF Expression

The mRNA expressions of BMP-2 in the control group (46 ± 5; 95% CI, 43–49) were lower (p < 0.001) than in the LIPUS group (75 ± 7; 95% CI, 70–79). The protein expression of BMP-2 in the control group (15 ± 2; 95% CI, 14–16) was lower (p < 0.001) than in the LIPUS group (30 ± 3; 95% CI, 28–31). However, VEGF mRNA expression was not different (p = 0.114; Table 2) between the LIPUS group (28 ± 2; 95% CI, 26–29) and the control group (26 ± 3; 95% CI, 24–28). VEGF protein expression also was not different (p = 0.0124, Fig. 6) between the LIPUS group (23 ± 6; 95% CI, 19–27) and the control group (22 ± 6; 95% CI, 18–26).

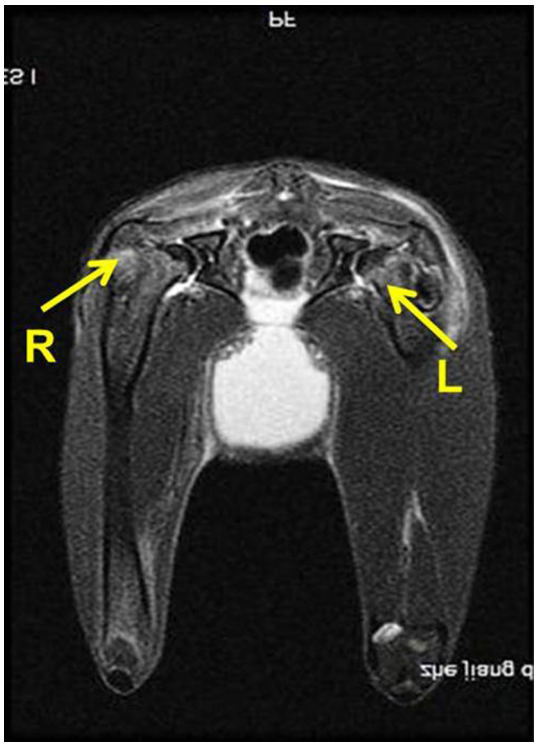

Fig. 4 This MR image obtained 2 weeks after methylprednisolone injection showed signs of edema (arrows) in the proximal femur. R = right side; L = left side.

Discussion

Although some studies document that steroids are a leading cause of femoral head osteonecrosis [1, 35, 41], the mechanisms of steroid-induced osteonecrosis remain unclear and there currently is no effective treatment for the disease. Therefore, a valid treatment is imperative for preventing collapse of the femoral head and subsequent osteoarthritis. Several studies have reported that LIPUS can enhance bone repair and local blood flow in animal models [3, 16, 24, 34]. However, whether the effect of osteogenesis and neovascularization by LIPUS can enhance the repair progress in steroid-associated osteonecrosis is unknown. To the best of our knowledge, our study is the first preclinical study to examine bone repair enhancement by LIPUS in an early-stage steroid-associated osteonecrosis rabbit model. The results confirm the hypothesis that LIPUS facilitates osteogenesis and neovascularization. In addition, we found that BMP-2 mRNA and protein expression were increased by LIPUS treatment.

Our study has some limitations. First, the dose-timing effects of LIPUS treatment were not assessed. Whether altered LIPUS signal parameters or longer treatment periods would have been more effective was considered to be beyond the scope of this study. Second, this steroid-associated osteonecrosis rabbit model is commonly used with a high incidence of osteonecrosis [26, 35–37]. However, osteonecrosis lesions do not lead to joint collapse in rabbits.

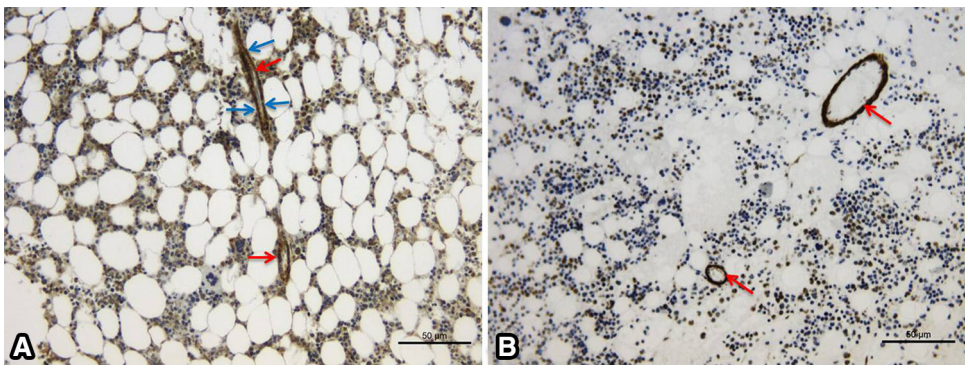

Fig. 5A–B Examples of α-SMA staining from (**A**) control group showed that the vessels (red arrows) became flattened, which were compressed by the enlarged fat cells (blue arrows) (Original magnification, × 200). (**B**) The vessels (red arrows) in the LIPUS group were normal (Original magnification, × 200).

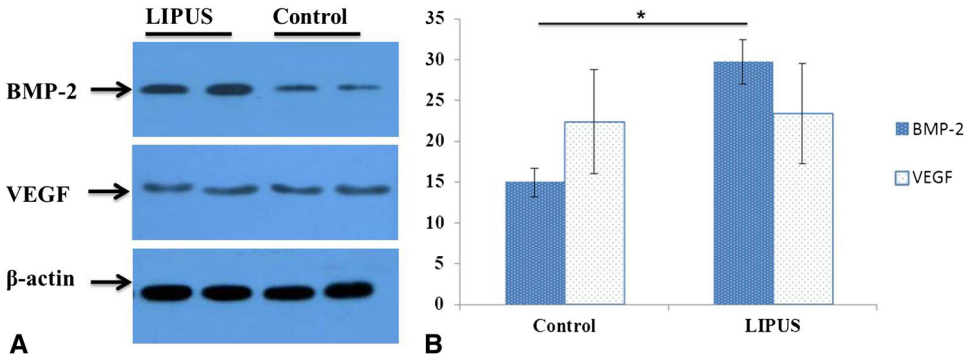

Fig. 6A–B (**A**) These band scans shows the Western blot analysis of BMP-2 and VEGF protein expression in the LIPUS and control groups. (**B**) The bar graph indicates the protein expression of BMP-2 in the LIPUS group was higher than in the control group ($p < 0.001$). However, there was no difference of VEGF protein expression between the two groups ($p = 0.0124$).

This could be attributable to dissimilarities in weightbearing between quadrupedal animals and bipedal humans, especially at the hip [26, 35]. Third, to keep the cost of the study manageable and avoid the additional factor of hormonal differences, only male rabbits were used in this study. Therefore, these results may not be generalizable to both sexes. Fourth, because there was no mineral apposition in the necrotic bone, the mineral apposition rate was measured only in the area of peripheral reconstruction. It may be not appropriate to show regeneration of necrotic bone, but it can indicate regeneration of the living bone, which mainly bears the weight during the repair progress of osteonecrosis.

We found that LIPUS can enhance the osteogenic effect and biomechanical strength. MSCs can differentiate into osteoblasts, which can facilitate new bone formation [35]. However, steroids can induce differentiation of MSCs into an adipocyte lineage, thereby inhibiting osteogenic differentiation [30]. The decreased activity of MSCs results in inadequate bone repair, which may be a triggering step leading to the onset and pathogenesis of steroid-associated osteonecrosis [13, 14]. The reduced trabecular bone volume, enlarged fat cells, and poor mechanical properties observed in steroid-associated osteonecrosis femoral heads are the result of reduced osteogenic differentiation and osteoblast activity [22, 36]. The current study revealed substantially lower percentages of empty lacunae, thicker trabecular bones, and smaller fat cells in the femoral heads in the LIPUS group, suggesting better bone repair in LIPUS-treated steroid-associated osteonecrosis. The improved loading strength as a result of LIPUS might reduce the incidence of femoral head collapse. Previous studies have found that LIPUS can enhance osteogenic differentiation of human MSCs and can accelerate osteoblast activity and bone formation [19, 34], which supports our findings. In addition, increased mineral apposition rate, osteoid thickness, and smaller fat cells denote intensified osteoblast activity and osteogenic differentiation [24, 29]. Thus, enhancement of osteogenesis by LIPUS might be explained by enhanced osteogenic capability in existing MSCs and enhanced osteoblast activity.

Neovascularization also was increased by LIPUS treatment. Osteogenesis and neovascularization play important roles during bone repair. In addition to the impaired activity of MSCs in the steroid-associated osteonecrosis rabbit model, it has been reported that there are effects on hematopoietic stem cells in this model [40]. Neovascularization is thought to be the result of hematopoietic stem cells and endothelial progenitor cell activity. The results of our study indicated that there were more blood vessels in LIPUS-treated limbs, which is in accordance with results of a previous study [3]. The enhanced neovascularization suggests that LIPUS can increase the activity of hematopoietic stem cells and improve local blood perfusion. Consistent with previous studies, we also found compression of blood vessels by enlarged bone marrow fat cells (Fig. 5A) in the control group, which could decrease blood perfusion and lead to ischemia [22, 30]. The decreased size of fat cells in LIPUS-treated limbs could decrease the intramedullary pressure and improve blood perfusion. However, there was no major difference in vessel diameter between limbs in the control group and the LIPUS group. This might be because there were more, and smaller, new vessels in LIPUS-treated limbs. Because sufficient blood flow is a fundamental prerequisite for bone repair [40], LIPUS may be a potential approach for improving treatment of early-stage steroid-associated osteonecrosis.

BMP-2 expression has been found to be substantially lower in femoral heads with steroid-associated osteonecrosis than in femoral heads of normal animals. It has been established that BMP-2 plays a central role in initiating bone formation [42], stimulating osteogenic differentiation of MSCs [9], and increasing osteoblast activity [10]. The lower BMP-2 expression could reduce local MSC activity and the capacity for bone repair [32]. In our study, LIPUS increased BMP-2 mRNA and protein expression in femoral heads with steroid-associated osteonecrosis. Therefore, it is possible that BMP-2 acts as a key regulator that promotes bone formation and repair processes in steroid-associated osteonecrosis. VEGF also plays an important role in normal and abnormal neovascularization [11, 12]. Prior studies have

shown that LIPUS stimulates the production of VEGF in vitro and in vivo [21, 27]. However, in our study there was no major difference in VEGF levels between the two groups. MRI for this animal model 2 weeks after methylprednisolone injection showed the appearance of edema in the proximal femur (Fig. 4). Because hypoxia is one of the most potent inducers of VEGF production [11], VEGF expression usually is increased in edematous areas of femoral heads with osteonecrosis femoral [8, 20]. Hypoxia might increase VEGF expression in this early-stage osteonecrosis. As the number of blood vessels increases owing to LIPUS treatment, blood perfusion would be enhanced and hypoxia would be gradually reduced, leading to a decrease in VEGF expression. This might neutralize any enhancement of VEGF expression caused by LIPUS. Cheung et al. [7] found that VEGF expression peaked 4 weeks after surgery in an osteoporotic fracture model. These findings may explain why there was no difference in VEGF expression between the two groups at 12 weeks in the current study. Future studies should examine the dynamic expression of VEGF at earlier times.

The results of our study support the prior hypothesis that LIPUS promotes bone repair and vascularization in a rabbit model of steroid-associated osteonecrosis [38]. This model is a prophylactic model because the LIPUS treatment was administered before osteonecrosis formation. Thus, these results show that LIPUS can prevent or delay the progression of steroid-associated osteonecrosis. If patients were to receive LIPUS treatment, it would be conducted before pulsed steroid therapy. Although LIPUS cannot completely stop the progression of steroid-associated osteonecrosis, it appears to enhance bone regeneration and vascularization in femoral heads with osteonecrosis, which might be beneficial for improving the bone repair of osteonecrosis. LIPUS has the potential to be a noninvasive, cost-effective treatment which can be administered in an outpatient setting. Future research could be directed toward such additional applications.

Acknowledgments We thank Jinfan Li MD and Lin Xu MD (Department of Pathology, Second Affiliated Hospital, School of Medicine, Zhejiang University), for histologic evaluation.

References

1. Amanatullah DF, Strauss EJ, Di Cesare PE. Current management options for osteonecrosis of the femoral head: part 1. Diagnosis and nonoperative management. *Am J Orthop (Belle Mead NJ).* 2011;40:E186–E192.
2. Barou O, Mekraldi S, Vico L, Boivin G, Alexandre C, Lafage-Proust MH. Relationships between trabecular bone remodeling and bone vascularization: a quantitative study. *Bone.* 2002;30: 604–612.
3. Barzelai S, Sharabani-Yosef O, Holbova R, Castel D, Walden R, Engelberg S, Scheinowitz M. Low-intensity ultrasound induces angiogenesis in rat hind-limb ischemia. *Ultrasound Med Biol.* 2006;32:139–145.
4. Boss JH, Misselevich I. Osteonecrosis of the femoral head of laboratory animals: the lessons learned from a comparative study of osteonecrosis in man and experimental animals. *Vet Pathol.* 2003;40:345–354.
5. Calder JD, Buttery L, Revell PA, Pearse M, Polak JM. Apoptosis: a significant cause of bone cell death in osteonecrosis of the femoral head. *J Bone Joint Surg Br.* 2004;86:1209–1213.
6. Chandra A, Lan S, Zhu J, Lin T, Zhang X, Siclari VA, Altman AR, Cengel KA, Liu XS, Qin L. PTH prevents the adverse effects of focal radiation on bone architecture in young rats. *Bone.* 2013;55:449–457.
7. Cheung WH, Chow SK, Sun MH, Qin L, Leung KS. Low-intensity pulsed ultrasound accelerated callus formation, angiogenesis and callus remodeling in osteoporotic fracture healing. *Ultrasound Med Biol.* 2011;37:231–238.
8. Clarkin CE, Gerstenfeld LC. VEGF and bone cell signalling: an essential vessel for communication? *Cell Biochem Funct.* 2013;31: 1–11.
9. Cui JH, Park K, Park SR, Min BH. Effects of low-intensity ultrasound on chondrogenic differentiation of mesenchymal stem cells embedded in polyglycolic acid: an in vivo study. *Tissue Eng.* 2006;12:75–82.
10. Doan N, Reher P, Meghji S, Harris M. In vitro effects of therapeutic ultrasound on cell proliferation, protein synthesis, and cytokine production by human fibroblasts, osteoblasts, and monocytes. *J Oral Maxillofac Surg.* 1999;57:409–419; discussion 420.
11. Ferrara N, Gerber HP, LeCouter J. The biology of VEGF and its receptors. *Nat Med.* 2003;9:669–676.
12. Gerber HP, Vu TH, Ryan AM, Kowalski J, Werb Z, Ferrara N. VEGF couples hypertrophic cartilage remodeling, ossification and angiogenesis during endochondral bone formation. *Nat Med.* 1999;5:623–628.
13. Glueck CJ, Fontaine RN, Gruppo R, Stroop D, Sieve-Smith L, Tracy T, Wang P. The plasminogen activator inhibitor-1 gene, hypofibrinolysis, and osteonecrosis. *Clin Orthop Relat Res.* 1999;366:133–146.
14. Hernigou P, Beaujean F, Lambotte JC. Decrease in the mesenchymal stem-cell pool in the proximal femur in corticosteroid-induced osteonecrosis. *J Bone Joint Surg Br.* 1999;81:349–355.
15. Hvid I, Hansen SL. Trabecular bone strength patterns at the proximal tibial epiphysis. *J Orthop Res.* 1985;3:464–472.
16. Ishihara Y, Ueki K, Sotobori M, Marukawa K, Moroi A. Bone regeneration by statin and low-intensity pulsed ultrasound (LIPUS) in rabbit nasal bone. *J Craniomaxillofac Surg.* 2014;42: 185–193.
17. Jones JP Jr, Ramirez S, Doty SB. The pathophysiologic role of fat in dysbaric osteonecrosis. *Clin Orthop Relat Res.* 1993;296:256–264.
18. Kerachian MA, Harvey EJ, Cournoyer D, Chow TY, Seguin C. Avascular necrosis of the femoral head: vascular hypotheses. *Endothelium.* 2006;13:237–244.
19. Khan Y, Laurencin CT. Fracture repair with ultrasound: clinical and cell-based evaluation. *J Bone Joint Surg Am.* 2008;90(suppl 1):138–144.
20. Li W, Sakai T, Nishii T, Nakamura N, Takao M, Yoshikawa H, Sugano N. Distribution of TRAP-positive cells and expression of HIF-1alpha, VEGF, and FGF-2 in the reparative reaction in patients with osteonecrosis of the femoral head. *J Orthop Res.* 2009;27:694–700.
21. Lovric V, Ledger M, Goldberg J, Harper W, Bertollo N, Pelletier MH, Oliver RA, Yu Y, Walsh WR. The effects of low-intensity pulsed ultrasound on tendon-bone healing in a transosseous-

equivalent sheep rotator cuff model. *Knee Surg Sports Traumatol Arthrosc.* 2013;21:466–475.
22. Miyanishi K, Yamamoto T, Irisa T, Yamashita A, Jingushi S, Noguchi Y, Iwamoto Y. Bone marrow fat cell enlargement and a rise in intraosseous pressure in steroid-treated rabbits with osteonecrosis. *Bone.* 2002;30:185–190.
23. Mont MA, Hungerford DS. Non-traumatic avascular necrosis of the femoral head. *J Bone Joint Surg Am.* 1995;77:459–474.
24. Ogawa T, Ishii T, Mishima H, Nishino T, Watanabe A, Ochiai N. Is low-intensity pulsed ultrasound effective for revitalizing a severely necrotic small bone? An experimental rabbit model. *Ultrasound Med Biol.* 2011;37:2028–2036.
25. Ortiguera CJ, Pulliam IT, Cabanela ME. Total hip arthroplasty for osteonecrosis: matched-pair analysis of 188 hips with long-term follow-up. *J Arthroplasty.* 1999;14:21–28.
26. Qin L, Zhang G, Sheng H, Yeung KW, Yeung HY, Chan CW, Cheung WH, Griffith J, Chiu KH, Leung KS. Multiple bioimaging modalities in evaluation of an experimental osteonecrosis induced by a combination of lipopolysaccharide and methylprednisolone. *Bone.* 2006;39:863–871.
27. Reher P, Doan N, Bradnock B, Meghji S, Harris M. Effect of ultrasound on the production of IL-8, basic FGF and VEGF. *Cytokine.* 1999;11:416–423.
28. Rubin C, Bolander M, Ryaby JP, Hadjiargyrou M. The use of low-intensity ultrasound to accelerate the healing of fractures. *J Bone Joint Surg Am.* 2001;83:259–270.
29. Rutten S, Nolte PA, Korstjens CM, van Duin MA, Klein-Nulend J. Low-intensity pulsed ultrasound increases bone volume, osteoid thickness and mineral apposition rate in the area of fracture healing in patients with a delayed union of the osteotomized fibula. *Bone.* 2008;43:348–354.
30. Sheng HH, Zhang GG, Cheung WH, Chan CW, Wang YX, Lee KM, Wang HF, Leung KS, Qin LL. Elevated adipogenesis of marrow mesenchymal stem cells during early steroid-associated osteonecrosis development. *J Orthop Surg Res.* 2007;2:15.
31. Uddin SM, Qin YX. Enhancement of osteogenic differentiation and proliferation in human mesenchymal stem cells by a modified low intensity ultrasound stimulation under simulated microgravity. *PLoS One.* 2013;8:e73914.
32. Wang W, Liu L, Dang X, Ma S, Zhang M, Wang K. The effect of core decompression on local expression of BMP-2, PPAR-gamma and bone regeneration in the steroid-induced femoral head osteonecrosis. *BMC Musculoskelet Disord.* 2012;13:142.
33. Wang Y, Yin L, Li Y, Liu P, Cui Q. Preventive effects of puerarin on alcohol-induced osteonecrosis. *Clin Orthop Relat Res.* 2008; 466:1059–1067.
34. Wu S, Kawahara Y, Manabe T, Ogawa K, Matsumoto M, Sasaki A, Yuge L. Low-intensity pulsed ultrasound accelerates osteoblast differentiation and promotes bone formation in an osteoporosis rat model. *Pathobiology.* 2009;76:99–107.
35. Xie XH, Wang XL, He YX, Liu Z, Sheng H, Zhang G, Qin L. Promotion of bone repair by implantation of cryopreserved bone marrow-derived mononuclear cells in a rabbit model of steroid-associated osteonecrosis. *Arthritis Rheum.* 2012;64: 1562–1571.
36. Xie XH, Wang XL, Zhang G, Liu Z, Yao D, Hung LK, Hung VW, Qin L. Impaired bone healing in rabbits with steroid-induced osteonecrosis. *J Bone Joint Surg Br.* 2011;93: 558–565.
37. Yamamoto T, Hirano K, Tsutsui H, Sugioka Y, Sueishi K. Corticosteroid enhances the experimental induction of osteonecrosis in rabbits with Shwartzman reaction. *Clin Orthop Relat Res.* 1995;316:235–243.
38. Yan SG, Huang LY, Cai XZ. Low-intensity pulsed ultrasound: a potential non-invasive therapy for femoral head osteonecrosis. *Med Hypotheses.* 2011;76:4–7.
39. Zhang G, Qin L, Sheng H, Wang XL, Wang YX, Yeung DK, Griffith JF, Yao XS, Xie XH, Li ZR, Lee KM, Leung KS. A novel semisynthesized small molecule icaritin reduces incidence of steroid-associated osteonecrosis with inhibition of both thrombosis and lipid-deposition in a dose-dependent manner. *Bone.* 2009;44:345–356.
40. Zhang G, Sheng H, He YX, Xie XH, Wang YX, Lee KM, Yeung KW, Li ZR, He W, Griffith JF, Leung KS, Qin L. Continuous occurrence of both insufficient neovascularization and elevated vascular permeability in rabbit proximal femur during inadequate repair of steroid-associated osteonecrotic lesions. *Arthritis Rheum.* 2009;60:2966–2977.
41. Zhao F, Li Z, Guo K. Clinical analysis of osteonecrosis of the femoral head induced by steroids. *Orthop Surg.* 2012;4: 28–34.
42. Zhao M, Xiao G, Berry JE, Franceschi RT, Reddi A, Somerman MJ. Bone morphogenetic protein 2 induces dental follicle cells to differentiate toward a cementoblast/osteoblast phenotype. *J Bone Miner Res.* 2002;17:1441–1451.
43. Zhao X, Cai XZ, Shi ZL, Zhu FB, Zhao GS, Yan SG. Low-intensity pulsed ultrasound (LIPUS) may prevent polyethylene induced periprosthetic osteolysis in vivo. *Ultrasound Med Biol.* 2012;38:238–246.